PHYSICAL REVIEW B VOLUME 17, NUMBER 8 15 APRIL 1978

Electrical properties of binary amorphous alloys

J. J. Hauser
Bell Laboratories, Murray Hill, New Jersey 07974

J. Tauc
Division of Engineering and Department of Physics, Brown University, Providence, Rhode Island 02912
(Received 21 November 1977)

Amorphous films of Au-Si, Mg-Zn, and Pt-Sb have been prepared by getter sputtering at 77°K over a wide range of compositions while the corresponding liquids can be quenched in the amorphous state only in a narrow range of compositions close to that of the eutectic. Their electrical resistance was measured in the temperature range 4.2–300°K. The results are compared with those obtained on similar liquid alloys and liquid quenched glasses. The resistivity and its temperature dependence are interpreted in terms of three scattering mechanisms: (a) Ziman theory, (b) structural defects, and (c) formation of covalent bonds, all of which being present in films, but (b) and (c) may be absent in bulk glasses and liquids. These differences in scattering account for the differences in electrical conduction of the three amorphous forms. Susceptibility measurements on amorphous Au-Si films and liquid Au-Si suggest a similarity between the amorphous and the liquid states. The present study would also suggest that while the eutectic composition is a crucial factor in obtaining an amorphous phase by quenching a liquid, it is not an important parameter in either the deposition of amorphous films or the properties of the amorphous phase.

I. INTRODUCTION

Amorphous metallic alloys can be produced by two different major methods: rapid quenching by splat cooling from the liquid state which yields what shall be referred to as a glass and vapor quenching from a vapor obtained by either evaporation or sputtering. Most of the metallic alloys suitable for the first method (i.e., the good glass formers) fall in two classes. In the first class, the alloy has the composition $M_{1-x}X_x$ (where M is a transition or noble metal and X is an element of column IV or V) with the concentration x in a narrow composition range near the eutectic.[1] Examples of such glasses are Au-Si,[2,3] Au-Pb,[4,5] Pd-Si,[6] and Pt-Sb.[7] In the second class M is an early transition metal with a less than half-filled d band (Ti, Zr, Nb, Ta) and X is a late transition metal with a nearly full d band (Cu, Ni) and x now spans a broader concentration range about the eutectic composition. Examples of the latter are Nb-Ni,[8] Ta-Ni,[8] and Zr-Cu.[9]

For the second method, Mader[10] suggested a rule to select elements likely to result in amorphous films: the atomic radii of the components should differ by about 10%. The range of compositions over which the amorphous state is obtained is greatest for the greatest difference in atomic radii.[10-12] This rule has been verified for several amorphous alloy films: Cu-Ag,[11] Co-Au,[13] Ag-X (where X= Fe, Co, Ni, or Gd),[14] to name only a few. As amorphous films can generally be obtained over a wider concentration range than glasses, it would be interesting to study whether an amorphous film with the eutectic composition has properties different from those of a noneutectic amorphous film. One would also like to compare the properties [resistivity, temperature coefficient of resistivity (TCR), x-ray structure, etc.] of an amorphous film with the corresponding glass. Furthermore, it has been reported[15] that some liquids (Fe-Ge, Ni-Ge) have a maximum in the resistivity and a negative TCR in a certain concentration range which includes in particular the eutectic composition. This behavior is by no means general since liquid Pd-Si has a positive TCR near the eutectic composition.[16] This therefore raises the following questions: To what extent does the amorphous phase resemble the liquid state, and more specifically, will the amorphous phase display a resistivity maximum and a negative TCR in the vicinity of the eutectic composition? It is the purpose of this study to answer some of these questions.

II. EXPERIMENTAL PROCEDURE

All alloy films of the present study were getter sputtered at 2.25 W (1500 V, 1.5 mA) with an argon pressure of approximately 3×10^{-2} Torr onto sapphire substrates held at 77°K. Most films are deposited for several hours (3–4) which resulted in film thicknesses ranging from 1 to 3 μm. Because of their greater resistance, a few thin Au-Si films (5 min depositions) were prepared to ascertain the TCR with greater precision; conversely the resistivity of such films is not as well determined because of the greater uncertainty in

 © 1978 The American Physical Society

TABLE I. Properties of Au-Si films.

Film	Rate (Å/min)	d (μm)	ρ_{77} (μΩ cm)	$[(dR/R)dT]_D$	$[(dR/R/dT]_A$
Si(7) No. 1[a]	199	1.89	27	...	...
Si(10) No. 1[a]	143	2.58	46	...	...
Si(11.5) No. 1[b]	120	2.16	71	$+8.4\times10^{-5}$	6.9×10^{-5}
No. 2[b]	162	2.92	46	$+8.8\times10^{-5}$	0
No. 3[b]	161	2.90	44	0	0
Si(13) No. 1	107	1.93	91	$+2.7\times10^{-4}$	...
No. 2	151	2.72	72	$+1.7\times10^{-4}$	-1.2×10^{-4}
No. 3	146	2.62	61	$+1.2\times10^{-4}$	$+1.3\times10^{-4}$
No. 5	239	0.12	77	$+1.1\times10^{-4}$	$+1.5\times10^{-4}$
No. 6	229	0.11	110	$+2.4\times10^{-4}$	...
Si(16) No. 1	97	1.16	86	-2.7×10^{-4}	-3.4×10^{-5}
No. 2	98	1.17	96	-8.3×10^{-5}	-1.2×10^{-4}
Si(19) No. 1	96	1.73	109	0	-2.3×10^{-4}
No. 2	143	2.57	102	0	-1.3×10^{-4}
No. 3	105	1.90	85	0	-9×10^{-5}
No. 6	212	0.11	150	0	-1.6×10^{-4}
No. 7	237	0.12	140	0	-2.4×10^{-4}
Si(23) No. 1	115	1.38	100	0	-1.3×10^{-4}
No. 2	92	1.11	108	0	-2.4×10^{-4}
Si(25) No. 1	71	1.71	115	0	...
No. 2	108	1.95	113	0	0
No. 3	94	1.69	112	0	-1.9×10^{-4}
No. 6	106	0.05	130	0	-1.8×10^{-4}
No. 7	103	0.05	74	0	-2.3×10^{-4}
Si(31) No. 1	122	2.93	108	0	...
No. 2	166	3.00	111	-3.7×10^{-5}	-2×10^{-4}
No. 3	153	2.76	120	0	-5.2×10^{-4}
Si(40) No. 1	119	2.14	177	-1.5×10^{-4}	-1.7×10^{-4}
No. 2	93	1.67	181	-8×10^{-5}	-3.1×10^{-4}
No. 3	97	1.74	202	-8×10^{-5}	-2.8×10^{-4}
Si(50) No. 1	130	3.13	213	-1.7×10^{-4}	-5.3×10^{-4}
No. 2	146	2.64	209	-6.9×10^{-5}	-1.5×10^{-4}
No. 3	117	2.11	217	-5.3×10^{-5}	-3.7×10^{-4}

[a]Crystalline as deposited.

[b]Amorphous as deposited; crystalline at room temperature.

the film thickness. The film thickness was determined from the weight gain using as a density a linear average of the densities of the constituent elements. The film thickness of a few Au-Si films was measured directly with a Sloane-Dektak step-measuring apparatus with the result that the error in the film thickness determined with the average density is less than 20%. The rates of deposition and the film thickness are listed for all three alloy systems in Tables I–III.

The sputtering targets were prepared in various ways. For Au-Si alloys, the required amounts of gold and silicon were melted inductively[17] in an alumina crucible under an argon atmosphere. The Mg-Zn targets were prepared[17] in essentially the same way. Since the mixing of Mg and Zn is particularly difficult because of the large density difference between the two metals, the best results were obtained by preparing a master alloy ($Mg_{0.95}Zn_{0.05}$);[18] higher Zn concentrations were obtained by remelting the master alloy with more Zn. Despite these precautions (master alloy, mixing by induction melting, and stirring) the mixing remained imperfect, and the composition of the films was determined with the help of x-ray fluorescence counts taken on the surfaces of the targets. The preparation of Pt-Sb alloys was hampered by the high vapor pressure of Sb at elevated temperatures. Homogeneous alloys were obtained by sealing the required amounts of Pt sponge and Sb powder in an evacuated quartz tube. The mixture was then heated in a furnace and air quenched.[19]

Following deposition the film is transferred under liquid nitrogen onto the four-probe resistivity holder, which is then immersed in liquid helium. The resistivity of the film is then measured in helium gas at atmospheric pressure as a function of temperature by warming to room temperature.

TABLE II. Properties of Mg-Zn films.

Film	Rate (Å/min)	d (μm)	ρ_{77} (μΩ cm)	$[(dR/R)/dT]_D$	$[(dR/R)/dT]_A$
Mg No. 1[a]	156	2.80	300	$+2.6\times10^{-4}$	...
No. 2[a]	156	2.80	240	$+3.2\times10^{-4}$	...
Zn(5) No. 1[a]	144	2.59	140	$+3\times10^{-4}$	$+1.8\times10^{-4}$
Zn(10) No. 1	127	2.29	110	$+2\times10^{-4}$	$+2.1\times10^{-4}$
No. 2	216	1.29	120	$+2.2\times10^{-4}$	$+2.5\times10^{-4}$
No. 3	121	3.63	120	$+2.1\times10^{-4}$	...
No. 4	137	1.64	110	$+1.7\times10^{-4}$	...
No. 5	133	0.40	120	$+3.6\times10^{-5}$	$+2.3\times10^{-4}$
Zn(30) No. 1	135	0.81	130	-3.4×10^{-4}	$+4.1\times10^{-5}$
				$+1.8\times10^{-4}$	...
No. 2	116	2.80	120	-2.7×10^{-4}	...
No. 5	126	0.38	96	$+1\times10^{-4}$	$+1.7\times10^{-4}$
				-1.1×10^{-4}	-1×10^{-4}
No. 6	124	0.37	106	0	-1×10^{-4}
No. 8	166	2.00	130	$+6.6\times10^{-5}$	$+2.5\times10^{-4}$
No. 9	189	0.95	134	0	$+1.2\times10^{-4}$
Zn(48) No. 1	149	1.79	160	-2.8×10^{-4}	-2.3×10^{-4}
				$+2.5\times10^{-4}$	...
No. 2	150	1.80	220	$+8.5\times10^{-5}$	-2.5×10^{-4}
Zn(62) No. 1	132	1.59	191	-2.5×10^{-4}	0
No. 2	152	1.82	249	-4×10^{-5}	-1×10^{-4}
Zn(70) No. 1	197	2.37	212	-3×10^{-5}	-2×10^{-4}
No. 2	201	2.41	283	-1.4×10^{-4}	0
Zn(72.5) No. 1	120	1.44	187	0	...
No. 2	142	1.70	250	-2.6×10^{-4}	...
Zn(90) No. 1	164	1.97	120	-2.8×10^{-4}	$+3\times10^{-4}$
Zn No. 1[a]	100	1.82	82	$+3.6\times10^{-4}$	...

[a]Crystalline as deposited.

The amorphous nature of the films was ascertained by an x-ray diffraction trace. For this purpose, the film was transferred under liquid nitrogen onto a cold copper finger partially immersed in a liquid-nitrogen bath contained in a polystyrene box; in this way the x-ray diffraction data can be obtained without warming the samples above 77 °K.

The $Au_{0.81}Si_{0.19}$ susceptibility sample was prepared by sputtering on a sapphire substrate kept at 77 °K, a film approximately 68 μm thick. The sample was then warmed to room temperature and scraped with fused quartz. The resulting powder was then placed in an ultrapure quartz container and measured by the Faraday method.[20] The amorphous structure of the sample was confirmed by an x-ray diffractometer trace obtained on a slurry of the powder prepared with Duco cement.

III. EXPERIMENTAL RESULTS AND DISCUSSION

A. Structural properties

As shown in Table I, Au-Si films with a Si content less than or equal to 10 at.% are crystalline even as deposited at 77 °K; films with 11.5 at.% are transitional, i.e., they are amorphous in the as-deposited state but crystalline when warmed

TABLE III. Properties of Pt-Sb films.

Film	Rate (Å/min)	d (μm)	ρ_{77} (μΩ cm)	$[(dR/R)dT]_D$	$[(dR/R)/dT]_A$
Sb(20) No. 1[a]	145	2.18	72	$+2.1\times10^{-4}$	...
No. 2[a]	125	2.25	75	$+2.9\times10^{-4}$	...
Sb(33) No. 1	134	2.42	111	-3×10^{-5}	$+2\times10^{-4}$
No. 2	115	2.08	110	0	$+1.7\times10^{-4}$
Sb(40) No. 1	135	2.43	118	0	-1.6×10^{-4}
No. 2	125	2.26	120	0	-1.4×10^{-4}

[a]Amorphous as deposited, crystalline at room temperature.

to room temperature, and films containing 13 at.% Si or more remain amorphous at room temperature. Actually the 13 at.% Si films are still somewhat transitional because although amorphous when warmed to room temperature, certain films did recrystallize after staying a few days at room temperature. On the other hand, films containing more than 13-at.% Si are truly stable at room temperature (still amorphous after a week); recrystallization starts above 373 °K (annealing for 15 min at 373 °K shows no sign of crystallinity) while recrystallization is complete after 20 min at 550 °K. Consequently, the amorphous Au-Si films are more stable than the amorphous splats which have a glass temperature T_g of about 290 °K and are therefore unstable at room temperature.[3] The greater stability of the films is undoubtedly caused by the incorporation of argon (≃1%) during deposition.

An example of crystallinity in an as-deposited film is shown in the top of Fig. 1. It is clear from Fig. 1 that crystallinity is easily detectable in Au-Si films, because such films have upon recrystallization a strong (111) preferred orientation which is typical in fcc films. Actually, crystallinity can also be detected by simple visual inspection: amorphous films have a silverlike sheen while crystalline films have a straw-colored (yellowish) reflection. One may object that this simple detection may overlook the presence of microcrystals smaller than the wavelength of light. The sharp transition from crystalline to amorphous as a function of Si content (≃11.5 at.%) argues to the contrary. It would seem that when the conditions of composition or temperature are such that recrystallization occurs, grain growth is fast enough to allow visual observation of the crystals.

An example of x-ray pattern for an amorphous Au-Si (*a*-Au-Si) film is shown in Fig. 1. The bottom trace was obtained on the as-deposited film at 77 °K and the middle trace after warming the film to room temperature. It is clear from the middle trace of Fig. 1 that there is no sign of crystallinity in the film at 300 °K [see the absence of even a 20-Hz structure at the (111) position as compared to the 800-Hz line shown in the top trace]. The main structure exhibited by both bottom traces in Fig. 1 is a wide peak centered at a 2θ value of 39.6°; since these patterns were obtained with Cu $K\alpha$ radiation, this 2θ value corresponds to $(\sin\theta)/\lambda = 0.22$, which is exactly the value reported for the center of the wide x-ray peak seen for a-$Au_{0.81}Si_{0.19}$ glass.[3] Consequently, it would seem, based on this coarse comparison, that an amorphous film is structurally similar to the corresponding glass. The same conclusion was recently reached on a-$Pd_{0.80}Ge_{0.20}$ where extended-

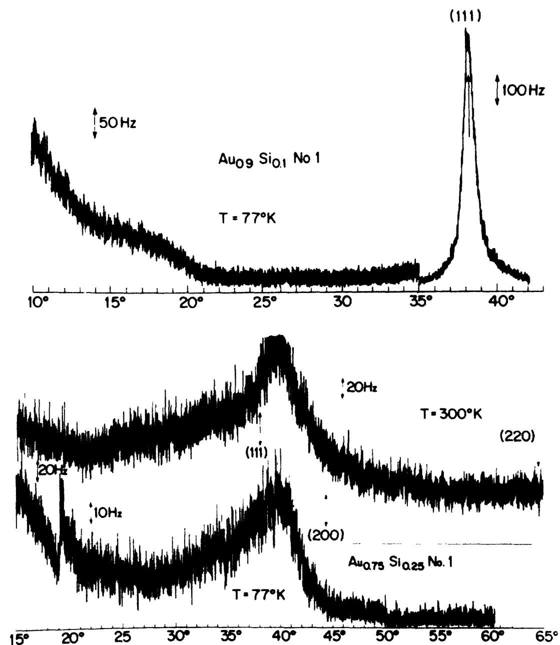

FIG. 1. X-ray diffractometer traces as a function of 2θ values (the arrows show the positions of the crystalline Au lines). The top trace refers to crystalline $Au_{0.9}Si_{0.1}$, the middle trace to a-$Au_{0.75}Si_{0.25}$ taken at 300 °K and the bottom trace to a-$Au_{0.75}Si_{0.25}$ taken at 77 °K. Note the change of ordinate scale on the bottom trace at $2\theta = 19$ °K.

x-ray-absorption fine-structure (EXAFS) measurements have shown that a Ge atom is surrounded by 8.6 ± 0.5 Pd atoms in both the *a*-film and the glass.[21] Besides the similar structure seen in the bottom two curves of Fig. 1 there are also dissimilarities: the pattern on the as-deposited film at 77 °K shows both a lower peak intensity over background and a larger relative intensity at low angles. The same general characteristics have been seen in many other amorphous metallic[14] and semiconducting[22,23] films and were attributed[22] to the more distorted structure in the as-deposited film. The same dissimilarity between an as-deposited film and a film annealed at 300 °K can be seen for the two compositions studied in the two top traces of Fig. 2. Furthermore, a comparison of Figs. 1 and 2 (which both show a wide peak centered at $2\theta = 39.6°$) suggests that the basic structure of *a*-Au-Si films remains the same as the Si content varies from 13 to 31 at.%. In particular one may conclude that *a*-films near or at eutectic composition (19 at.% Si) are not structurally different from *a*-films with other compositions. On the other hand, when the Si content exceeds 40 at.%, one notices a major modification in the x-ray pattern which is illustrated in the bottom trace of Fig. 2 for *a*-

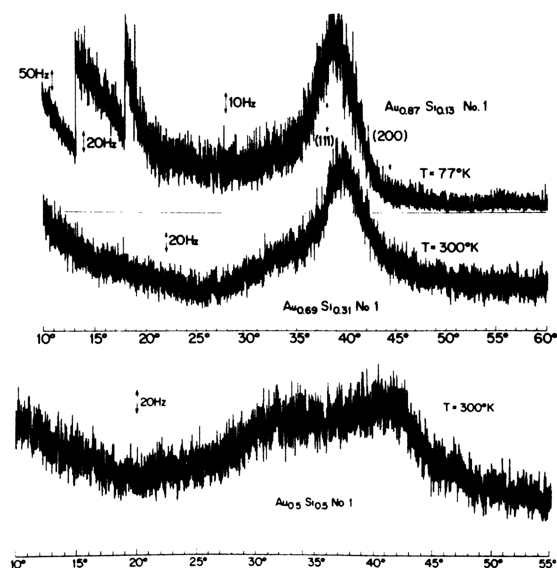

FIG. 2. X-ray diffractometer traces as a function of 2θ values. Top trace for $Au_{0.87}Si_{0.13}$ taken at 77 °K (note the changes of ordinate scale at $2\theta = 13.2°$ and 18°); middle trace for $Au_{0.69}Si_{0.31}$, and bottom trace for $Au_{0.5}Si_{0.5}$.

$Au_{0.5}Si_{0.5}$. This structural change is accompanied by a large increase in the resistivity (see Table I) and can be understood in terms of the increasing number of tetrahedrally coordinated Si atoms (see

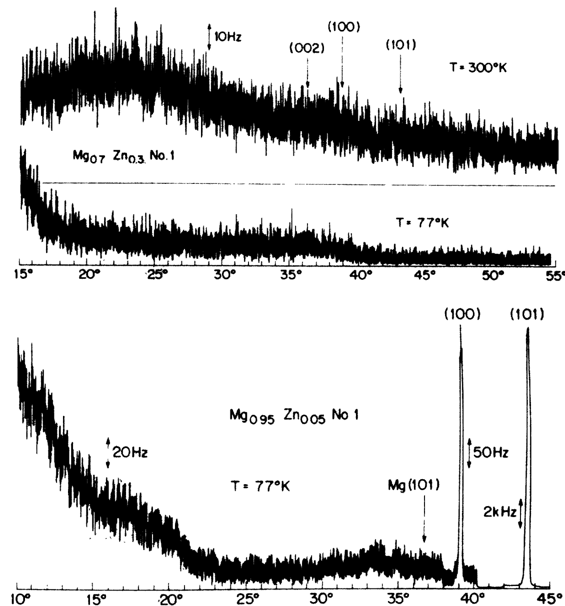

FIG. 3. X-ray diffractometer traces. Bottom trace on a deposited film at 77 °K showing two Zn diffraction lines (note the changes of ordinate scale at $2\theta = 38°$ and 40°); the two top traces refer to a-$Mg_{0.70}Zn_{0.30}$ taken at 77 K and 300 °K.

the discussion on electrical properties in Sec. III B).

The x-ray properties of the two other alloy systems are essentially the same as those for Au-Si and will be discussed very briefly. As shown by Table II, one can prepare a-Mg-Zn films over a very wide compositional range, i.e., as little as 10 at. % of one element in the other is sufficient to produce an a-film. This is quite consistent with Mader's rule[10] since the difference in Goldschmidt radii[24] is 16% for the Mg-Zn system as compared to 9% for the Au-Si system. An example of crystallinity in an as-deposited film can be seen from the two crystalline Zn lines shown in the bottom trace of Fig. 3. Although Mg diffraction lines cannot be seen because of the very low scattering intensity of Mg, it is clear from Fig. 3 that it is very easy to detect microcrystallinity if present at all. Indeed, as shown in Fig. 3, even with a Zn concentration as low as 5 at. %, the (101) diffraction line is extremely intense (17000 Hz) because the film has a strong (101) (type-I pyramidal plane) preferred orientation. The absence of crystallinity in an a-Mg-Zn film of eutectic composition is shown in Fig. 6 by the two top traces. As shown by Table III, the study of Pt-Sb films was very brief and their x-ray structure will therefore be omitted.

B. Electrical properties

The resistivity was measured on all alloy systems on the as-deposited films at 77 °K; the film was then cooled to 4.2 °K and the TCR, $(dR/R)/dT$, was obtained on the unannealed film (subscript D in Tables I–III). The film was then warmed to room temperature and the TCR remeasured on the annealed film (subscript A in Tables I–III). Although all the values of resistivity and TCR are listed for the three-alloy systems in Tables I–III, the dependence of these properties on composition is best studied in the corresponding plots (Figs. 4 and 6). The dependence of the resistivity at 77 °K on silicon concentration is shown for Au-Si films in the bottom of Fig. 4. It should be mentioned that the values of the resistivity listed in Table I for thin films (500–1200 Å) were omitted from Fig. 4, because the resistivity of such films suffers from a large uncertainty (15%–30%) in film-thickness determination. On the other hand, such films yield very reliable TCR values because of their high resistance. It is also clear from Table I that both the resistivity and the TCR are independent of film thickness. The most significant features of the data shown in Fig. 4 are the rapid increase in resistivity in the transition region between crystalline and amorphous films followed by a leveling-off

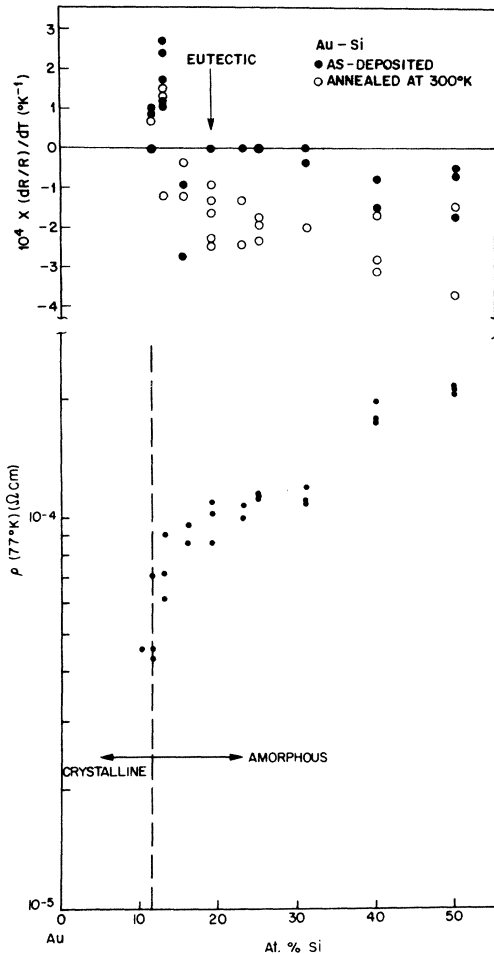

FIG. 4. Bottom: dependence of the resistivity measured on as-deposited films [$\rho(77\,°K)$] on silicon concentration. Top: dependence of the temperature coefficient of resistivity on silicon concentration.

with no extremum in the vicinity of the eutectic composition (~19 at.%). There is also a significant increase in resistivity above 40 at.% Si.

In certain liquids, a maximum in the resistivity has been explained in terms of a modified Ziman theory[15] and is supposed to occur when $2k_F = q_p$ [where k_F is the Fermi momentum and q_p is the value of q corresponding to the first peak in the structure factor $S(q)$]. One should also point out that the composition corresponding to this maximum is very close to the eutectic composition.

The absence of a maximum near the eutectic composition (Fig. 4) may be caused by three distinct mechanism. First, the maximum may not be a general property of all liquids and in particular may or may not occur in liquid Au-Si.[25] Second, an extra scattering mechanism may occur in films as a result of some defects introduced during film deposition. This defect scattering can, however, be ruled our for a-Au-Si films since the resistivity of liquid $Au_{0.81}Si_{0.19}$ at the melting point[25] is about 100 $\mu\Omega$ cm, which is very close to the value reported for a-Au-Si films (Table I and Fig. 4). Third, there is a fundamental difference between the coordination of Si in the liquid and in the amorphous film. In the liquid, the Si has metallic coordination at all Si concentrations while it becomes tetrahedrally coordinated for high Si concentration (≃30–40 at.%) in the a-films. This tetrahedral coordination is evidenced both structurally (change in x-ray pattern discussed in Sec. III A) and by the increase in resistivity at 40 at.% (Fig. 4). This increase in resistivity is the precursor to the much larger increase which will occur at higher Si concentrations when the resistivity will enter the hopping regime.[26] This increase in resistivity stemming from the tetrahedrally coordinated Si atoms could conceivably overshadow the presence of a maximum. On the other hand, the value of the resistivity in the plateau of Fig. 4 (≃100 $\mu\Omega$cm) is in excellent agreement with the resistivity of other glasses [95 $\mu\Omega$cm for $Pd_{0.775}Cu_{0.06}Si_{0.165}$ (Ref. 27) and 80 $\mu\Omega$cm for $Pd_{0.81}Si_{0.19}$ (Ref. 16)] and liquids [100 $\mu\Omega$cm for $Au_{0.81}Si_{0.19}$ (Ref. 25), 95 $\mu\Omega$cm for $Pd_{0.81}Si_{0.19}$ (Ref. 16), and 100 ± 20 $\mu\Omega$cm for Ni-Ge (Ref. 15)]. Further correlations with the liquid can be reached by examining the concentration dependence of the TCR shown in the top of Fig. 4.

Despite the scatter of the data shown in the top of Fig. 4 (which in part may be due to some contribution by defect scattering), it is clear that the TCR for both as-deposited and annealed films becomes zero or negative (with an average value of $-2\times10^{-4}\,°K^{-1}$) for a silicon concentration equal to or greater than 16 at.%. This value of 16% where the TCR changes sign is close enough to the eutectic value (19%) to correlate the change of sign with the eutectic composition as can be done in certain liquids.[15] Furthermore, the values of TCR shown in Fig. 4 which correspond to variations of $d\rho/dT$ between $+3\times10^{-8}$ and -8×10^{-8} Ωcm °K^{-1} are in excellent agreement with the value of -2×10^{-8} Ωcm K^{-1} measured[25] on liquid $Au_{0.81}Si_{0.19}$ and with variations of $d\rho/dT$ observed in other liquids.[15]

Recently, theoretical models based on modified Ziman liquid-metal theory[28,29] have been proposed to explain the resistivity and the TCR of amorphous alloys. Although these theories are consistent with the order of magnitude of ρ and the change of sign of the TCR, they may not explain certain properties observed in a-films (such as the scatter in the TCR observed in a-Mg-Zn films) because they do not take into account covalent bonding or defect scattering. A model based on atomic

tunneling[30,31] may be applicable to a-films. As the structural disorder could conceivably vary from sample to sample as a result of slight variations in the deposition parameters, one could expect similar variations in the electrical properties.

Before discussing the concentration dependence of ρ and TCR for Mg-Zn alloys it is necessary to discuss the method used to determine the concentration of such alloys because of the poor mixing of the constitutent elements. It is well known that the concentration of a sputtered film is very close to that of the target,[14,32] and the problem of knowing the composition of a film is therefore reduced to establishing the composition of the target. The composition of the targets was determined by the x-ray fluorescence data shown in Fig. 5. The x-ray fluorescence counts shown in Fig. 5 were obtained on targets where the counts (both Zn and Mg) on both sides of the target did not differ by more than 20%; the average of both sides was then plotted versus the nominal concentration. The composition of other targets was established by obtaining the x-ray fluorescence counts on the sputtering face of the target and reading the composition from Fig. 5. The solid lines averaging the data shown in Fig. 5 give very plausible results. The Zn line comes very close at 100% Zn to the datum point actually measured on pure Zn and passes at 1% through 160 counts which correspond to 1.5% of the counts obtained on pure Zn. The Mg line, which was forced to pass through zero Mg count at 100% Zn, passes through the 180 counts measured on pure Mg at 0.76 at. % Zn which is again reasonable. One may therefore conclude from Fig. 5 that the absolute composition is known with an accuracy better than ±20%. The concentration dependence of ρ and TCR for Mg-Zn alloys is summarized in Table II where it can be seen that these properties are independent of thickness. The dependence of the resistivity at 77 °K on Zn concentration for Mg-Zn films is shown in the bottom of Fig. 6. The main features of interest for the data pertaining to amorphous films are the absence of an extremum at the eutectic composition (just as in the Au-Si system) and the presence

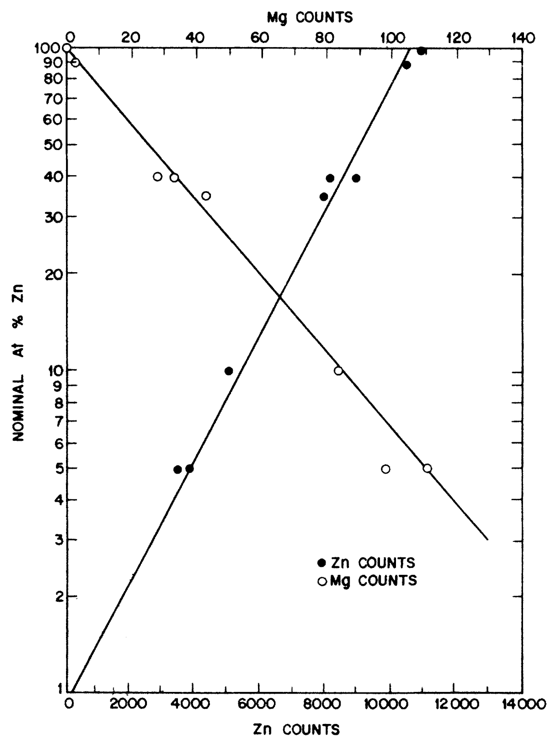

FIG. 5. Nominal Zn concentration of the target as a function of both Mg and Zn x-ray fluorescence counts.

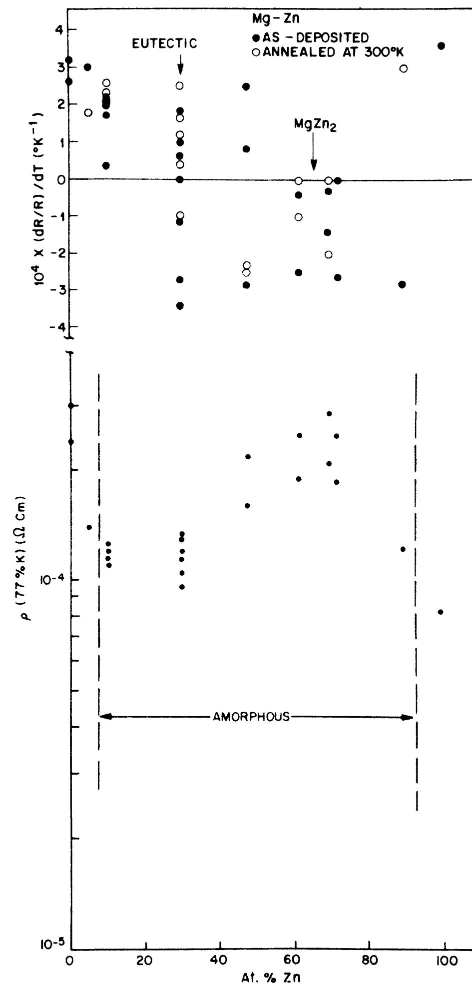

FIG. 6. Bottom: dependence of the resistivity measured on as-deposited films [(ρ(77 °K)] on zinc concentration. Top: dependence of the temperature coefficient of resistivity (TCR) on zinc concentration.

of a maximum near the concentration of the compound $MgZn_2$. These features are somewhat corroborated by the concentration dependence of the TCR shown in the top of Fig. 6. Indeed, the eutectic composition is only characterized by a large scatter in the sign and magnitude of the TCR (although one could argue that the first appearance of negative TCR occurs at this composition) while the concentration region near $MgZn_2$ is distinguished by the presence of a zero or negative TCR.

Although the absence of maximum can be explained by any of the three mechanisms proposed for a-Au-Si films, the scatter of the TCR would suggest that defect scattering may be particularly important for a-Mg-Zn films. Again the values of the resistivity and TCR are comparable to those reported in liquids.[15,16] The maximum in ρ and the negative TCR associated with $MgZn_2$ suggest the two following remarks. First, variations of ρ and TCR in amorphous films linked with the composition of a compound have been reported previously in Mg_3Sb_2,[33] GaSb,[34] and SiC,[35] to name only a few. Second, a eutectic is often very close in composition to a compound and one wonders whether a resistivity maximum reported in conjunction with a eutectic is not really linked with the compound. For example, the composition (33 at.% Ge)[15] corresponding to the maximum in ρ for liquid Fe-Ge is closer to Fe_2Ge than to the eutectic[36] (29%). Similarly, the maximum in ρ for liquid Ni-Ge occurs at 35 at.% Ge,[15] which is closer to the ϵ phase than to the eutectic[37] (28%). Furthermore, in the case of the Pd-Si system where no compound is reported in the vicinity of the eutectic composition,[38] the TCR of the liquid is positive.[16]

Before leaving the Mg-Zn system, one should stress two interesting features. First, this system is different from the glass formers discussed in the Introduction in the sense that it contains no transition metal. Furthermore, while the glass is only stable in the vicinity of the eutectic composition,[39] the amorphous films can be obtained over almost the whole compositional range (Table II). As in the present case the bonding remains metallic for all compositions (which was not the case for example in the Au-Si system for high Si concentrations), one would expect the resistivity of a-Mg-Zn films to differ from that of liquid Mg-Zn alloys only by the amount of scattering resulting from structural defects.

Finally, from the brief study performed on Pt-Sb alloys, which is summarized in Table III, one may draw similar conclusions to those previously described. Namely, the values of ρ ($\simeq$100 $\mu\Omega$cm) and TCR ($\simeq\pm 2\times 10^{-4}\,{}^\circ K^{-1}$) are similar to those measured on Au-Si and Mg-Zn. Again, there does not seem to be a resistivity maximum near the eutectic composition[7] ($\simeq$32 at.% Sb), while the TCR seems to become negative for Sb concentrations slightly larger than eutectic.

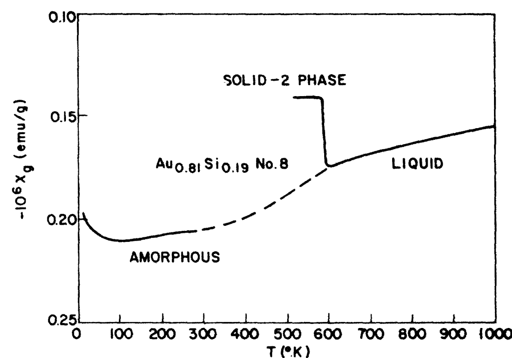

FIG. 7. Variation of the diamagnetic susceptibility of amorphous, liquid, and crystalline two-phase solid with temperature.

C. Magnetic susceptibility

The temperature dependence of the magnetic susceptibility of liquid $Au_{0.81}Si_{0.19}$ has been previously reported.[40] These data are shown as the solid curve in the upper right-hand corner of Fig. 7. Although hard to see from the figure, the slope ($d\chi_g/dT$) steepens below the liquidus temperature (636 °K). The liquid can actually be supercooled about 40 °K and freezes into a two-phase solid, which is accompanied by a rapid increase of the susceptibility to a value which remains temperature independent down to room temperature (solid square in Fig. 7). The diamagnetic susceptibility of an a-$Au_{0.81}Si_{0.19}$ film[41] is shown by the solid curve in the lower left-hand side corner of Fig. 7. The increase χ_g at low temperatures is due to a low level of paramagnetic impurities. The broken line shown in Fig. 7 suggests that the susceptibility of the amorphous film is in good agreement with a reasonable extrapolation of the susceptibility of the liquid in general and of the supercooled liquid in particular. The data shown in Fig. 7 suggest, therefore, that the amorphous phase is quite similar to the liquid.

IV. CONCLUSIONS

The amorphous phase seems to have intrinsic structural and electrical properties irrespective of the method of preparation (glass versus amorphous films). Indeed, the x-ray patterns of Au-Si films are similar to those reported for the glass[3] and the same was recently observed by EXAFS measurements on the Pd-Ge system.[21] The electrical properties of a-films are quanti-

tatively similar to those of glasses.[16,27] Furthermore, if one ignores possible differences in coordination for such atoms as Si or Ge at high Si or Ge concentrations, it would seem that the amorphous phase and the liquid phase are quite similar: the magnitudes of ρ and TCR are similar[15,16,25] and the susceptibilities of amorphous Au-Si and amorphous Pd-Si are in good agreement with extrapolations of the liquid susceptibility.[16]

There are, however, slight differences between a-films and liquids: although a change of sign of the TCR can be linked with the eutectic composition, there is no corresponding maximum in the resistivity. The absence of a maximum could be caused by three effects: absence of a maximum in the corresponding liquid, structural defect scattering, and covalent bonding. At any rate, although the glass-forming tendency is greatly increased in the vicinity of a deep eutectic,[42,43] the eutectic composition does not seem to have a marked effect on the structural or electrical properties of the amorphous phase.

More pronounced effects can be observed linking a maximum in ρ and a change of sign of the TCR with the presence of a compound ($MgZn_2$). Because of the proximity in compostion of many eutectics and compounds, one should be careful before attributing to the eutectic an anomaly in ρ or TCR. It would, of course, be better to obtain electrical data on the amorphous and liquid phases of the same system and as a result electrical measurements on liquid Au-Si have been undertaken.[25] The understanding of amorphous Au-Si alloys will also be enhanced by a study of the optical properties which have been already briefly discussed.[44]

ACKNOWLEDGMENTS

We would like to thank F. J. DiSalvo for the susceptibility measurements and C. M. Antosh, J. E. Bernardini, V. G. Lambrecht, and J. V. Waszczak for their technical assistance. We would also like to acknowledge discussions with E. Hauser.

---

[1]P. Duwez, ASM Trans. Q. 60, 607 (1967).
[2]W. Klement, Jr., R. H. Willens, and P. Duwez, Nature 187, 869 (1960).
[3]H. S. Chen and D. Turnbull, J. Appl. Phys. 38, 3646 (1967).
[4]P. K. Srivastava, B. C. Giessen, and N. J. Grant, Acta Metall. 16, 1199 (1968).
[5]P. Predecki, B. C. Giessen, and N. J. Grant, Trans. Metall. Soc. AIME 233, 1438 (1965).
[6]P. Duwez, R. H. Willens, and R. C. Crewdson, J. Appl. Phys. 36, 2267 (1965).
[7]P. K. Strivastava, B. C. Giessen, and N. J. Grant, Metall. Trans. 3, 977 (1972).
[8]R. C. Ruhl, B. C. Giessen, M. Cohen, and N. J. Grant, Acta Metall. 15, 1693 (1967).
[9]R. Ray. B. C. Giessen, and N. J. Grant, Scr. Metall. 2, 357 (1968).
[10]S. Mader, J. Vac. Sci. Technol. 2, 35 (1965).
[11]S. Mader, A. S. Nowick, and H. Widmer, Acta Metall. 15, 203 (1967).
[12]S Mader and A. S. Nowick, Acta Metall. 15, 215 (1967).
[13]S. Mader and A. S. Nowick, Appl. Phys. Lett. 7, 57 (1965).
[14]J. J. Hauser, Phys. Rev. B 12, 5160 (1975).
[15]G. Busch and H.-J. Güntherodt, in *Solid State Physics*, edited by H. Ehrenreich, F. Seitz, and D. Turnbull (Academic, New York, 1974), Vol. 29, p. 235.
[16]H.-J. Güntherodt, H. U. Künzi, M. Liard, M. Müller, R. Müller, and C. C. Tsuei, in *Second International Symposium on Amorphous Magnetism, Troy, New York, 1976*, edited by R. A. Levy and R. Hasegawa (Plenum, New York, 1977).
[17]We are indebted to J. E. Bernardini for the preparation of the Au-Si and Mg-Zn targets.
[18]We are indebted to J. H. Wernick for suggesting this idea.
[19]We are indebted to V. G. Lambrecht for the preparation of the Pt-Sb targets.
[20]F. J. DiSalvo, B. G. Bagley, R. S. Hutton, and A. H. Clark, Solid State Commun. 19, 97 (1976).
[21]T. M. Hayes, J. W. Allen, J. Tauc, B. C. Giessen, and J. J. Hauser (unpublished).
[22]J. J. Hauser and A. Staudinger, Phys. Rev. B 8, 607 (1973).
[23]J. J. Hauser, Phys. Rev. B 11, 3860 (1975).
[24]R. P. Elliot, *Constitution of Binary Alloys, First Supplement* (McGraw-Hill, New York, 1965), p. 872.
[25]The resistivity of liquid Au-Si alloys is currently under investigation by E.Hauser, S. Ray, and J. Tauc.
[26]J. J. Hauser, Phys. Rev. B 8, 3817 (1973).
[27]B. G. Bagley and F. J. DiSalvo, in *Amorphous Magnetism*, edited by H. O. Hooper and A. M. deGraaf (Plenum, New York, 1973), p. 143.
[28]S. R. Nagel, Phys. Rev. B 16, 1694 (1977).
[29]P. J. Cote and L. V. Meisel, Phys. Rev. Lett. 39, 102 (1977).
[30]C. C. Tsuei, Bull. Am. Phys. Soc. 22, 322 (1977).
[31]R. W. Cochrane, R. Harris, J. O. Ström-Olson, and M. J. Zuckermann, Phys. Rev. Lett. 35, 676 (1975).
[32]J. J. Hauser, Phys. Rev. B 9, 2544 (1974).
[33]R. Ferrier and D. J. Herrell, J. Non-Cryst. Solids 2, 278 (1970).
[34]J. J. Hauser, Phys. Rev. B 11, 738 (1975).
[35]J. J. Hauser, Philos. Mag. 35, 1557 (1977).
[36]M. Hansen, *Constitution of Binary Alloys*, second edition (McGraw-Hill, New York, 1958), p. 658.
[37]Ref. 36, p. 769.
[38]Ref. 36, p. 1126.
[39]A. Calka, M. Madhava, D. E. Polk, B. C. Giessen,

H. Matyja, and J. Vander Sande, Scr. Metall. 11, 65 (1977).
[40]B. G. Bagley, and F. J. DiSalvo, Bull. Am. Phys. Soc. 21, 385 (1976).
[41]We are indebted to F. J. DiSalvo and J. V. Waszczak for performing this measurement.
[42]D. Turnbull and M. H. Cohen, J. Chem. Phys. 34, 120 (1961).
[43]H. S. Chen, Acta Metall. 22, 1505 (1974).
[44]E. Hauser, J. Tauc, and J. J. Hauser, Bull. Am. Phys. Soc. 22, 335 (1977).